Proceedings of the 3rd International Conference on Advances in Energy Research and Applications (ICAERA'22)
~~Seoul, South Korea~~ Virtual Conference – October 27-29, 2022
Paper No. 113
DOI: 10.11159/icaera22.113

Transient Analysis of Lower and Ground Zone Energy Extraction in Solar Ponds with Temperature Drop across Exchangers

Sunirmit Verma[1], Ranjan Das[2]
Department of Mechanical Engineering, Indian Institute of Technology Ropar, Punjab, 140001, India
[1]E-mail: 2018mez0008@iitrpr.ac.in, Telephone: +91-7973848360
[2]E-mail: ranjandas@iitrpr.ac.in, Telephone: +91-1881-232372

Abstract - Solar ponds involve energy extraction generally from their lower convective zone. Sometimes, energy is extracted from ground below them too, in order to enhance the output. A transient model is presented that studies such a pond system. The novelty lies in the fact that temperature drop across exchanger surfaces in the two zones are included into the relevant equations, which has not been considered in earlier transient models. A transient analysis for a one-year period under the climatic conditions of Copiapo, Chile has been carried. The finite difference method has been used to solve the relevant equations via a MATLAB code. The model is successfully validated with a simpler version available in the literature. It has been shown that not considering this effect leads to a significant overestimation of the performance. A maximum error of about 13% is seen in the value of outlet temperature of the extracted water stream. Further, it is observed that exchanger pipes in the ground should be of as little cross section as possible. It is also seen that places where year average ambient temperature ground isotherm is deeper prove more productive for such pond systems. Finally, it is observed that mass flux corresponding to ground energy extraction should be low from outlet temperature point of view but should be higher from outgoing energy perspective.

***Keywords*:** solar pond; transient state; storage zone; ground; extraction; numerical solution

1. Introduction

The present era calls for urgent necessity towards harvesting of renewable energy in order to fulfil ever increasing global energy demand. These sources shall practically never cease to exist, cause lesser environmental degradation, and also require lesser maintenance as compared to their fossil-based counterparts. However, they do have their limitations. These are high initial costs, intermittent availability and dependence on geographical locations. Solar and geothermal are two forms of renewable energy that are readily available at most places on the planet. Hybridization of these two resources is preferable for improvement in the energy output from a system operated with just a single resource. It is therefore, no surprise that many studies have been conducted to analyse the performance of combined solar and geothermal systems. Few of these published during the recent few years have been discussed below.

Hammadi [1] combined a ground heat exchanger with a solar still via a transient model, and quantified the improvement in fresh water production through it. He obtained about 45 % enhancement. Assad *et al*. [2] investigated the combination of a parabolic trough collector and a steam geothermal power plant using System Advisor Model (SAM) software. Yang and Duan [3] used the artificial neural network technique to model the behaviour of a hybrid solar -geothermal system for a period of three decades. The combined system was shown to produce 17% more electricity than individual geothermal system. Li *et al*. [4] did an experimental work on the coupled system of solar chimney and earth air exchanger. They ignored thermal recovery of soil around the earth air exchanger and thus, their work was valid only for short time periods. Duarte *et al*. [5] studied a series connection of a ground water aquifer and a solar collector under Brazilian climate. Using lumped modelling method, a thermal as well as economic analysis was carried. Long *et al*. [6] carried numerical simulations for the integrated system of solar chimney and earth air exchanger. They used a combined TRANSYS -MATLAB based model and showed that a number of such hybrid systems are needed to achieve the required level of comfort conditioning that they aimed at achieving.

Salt gradient solar ponds are large size thermal reservoirs that serve both thermal energy storage and extraction purposes. They use a well-established and maintained salinity gradient for their functioning [7]. Their performance gets jeopardized by energy losses from surface [8], turbidity effect [9] and wall losses [10]. These can be regulated by use of covers, chemical

agents and insulation, respectively. Though not many, few studies combining solar ponds and ground exchangers are also available in the literature. For instance, Ganguly *et al*. [11] combined a solar pond and a vertical geothermal exchanger using a transient model. Verma and Das [12] gave an analytical model for optimisation of a solar pond suffering energy extraction from non-convective zone (NCZ), lower convective zone (LCZ) and neighbouring ground. Verma and Das [13] modified the work of Ganguly *et al*. [11] by taking temperature drop across exchangers in both the pond and the ground. However, their model had a drawback that it was a steady one.

It is observed that many researches on hybrid solar-geothermal systems exist in the literature, yet the combination of a solar pond and a geothermal exchanger has been investigated by very few. Out of all these works, none has given consideration to temperature drop across ground exchanger surface through a transient model. Transient analysis is more appropriate here because weather data pertaining to such systems invariably vary with time. Furthermore, consideration of finite effectiveness across the energy exchanging device will yield outputs which will be closer to an actual situation. In this work, the authors have eliminated this research gap by incorporating both these features in their simulation: transient behaviour as well as finite ground exchanger effectiveness.

2. Mathematical Model

Figure 1 represents the diagram of a solar pond system considered here. 10 exchanger pipes are installed in the LCZ and ground below as shown. Water enters them at instantaneous ambient temperature at all times. Energy losses from surface are considered but not from side walls, thus model is one dimensional in space. Thermophysical properties of water and ground are taken to be constants.

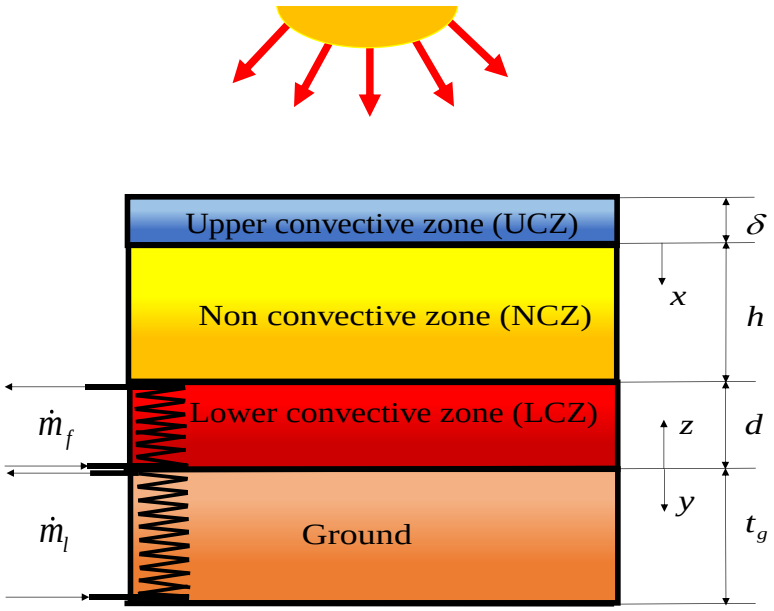

Figure 1: Schematic of a solar pond with ground energy extraction

Under the mentioned assumptions and taking *x*, *y*, *z*, to represent coordinates as shown in Figure 1, energy balance for differential elements in *NCZ*, *LCZ* exchanger stream, ground, and the ground exchanger stream provide 4 coupled partial differential equations [13, 14], which are written below in discretised form,

$$\frac{(T_n)_{i+1}^{\ j}+(T_n)_{i-1}^{\ j}-2(T_n)_i^j}{(\Delta x)^2}+\frac{I\beta_0}{k_n\{(i-1)dx+\delta\}}=\frac{\rho_n c_{pn}}{k_n}\left\{\frac{(T_n)_i^{\ j}-(T_n)_i^{\ j-1}}{\Delta t}\right\} \tag{1}$$

$$\frac{2\pi r_f n_f U_f}{\dot{m}_f c_{pf}}\left\{(T_n)_N^j-(T_f)_i^j\right\}-\left\{\frac{(T_f)_i^j-(T_f)_{i-1}^j}{\Delta z}\right\}=\frac{\rho_f \pi r_f^2 n_f}{\dot{m}_f}\left\{\frac{(T_f)_i^j-(T_f)_i^{j-1}}{\Delta t}\right\} \tag{2}$$

$$\frac{(T_g)_{i+1}^j+(T_g)_{i-1}^j-2(T_g)_i^j}{(\Delta y)^2}-\frac{2\pi r_g n_g U_g}{k_g A}\left\{(T_g)_i^j-(T_l)_i^j\right\}=\frac{\rho_g c_{pg}}{k_g}\left\{\frac{(T_g)_i^j-(T_g)_i^{j-1}}{\Delta t}\right\} \tag{3}$$

$$\frac{2\pi r_l n_l U_l}{\dot{m}_l c_{pl}}\left\{(T_g)_i^j-(T_l)_i^j\right\}+\left\{\frac{(T_l)_i^j-(T_l)_{i-1}^j}{\Delta y}\right\}=\frac{\pi r_l^2 n_l \rho_l}{\dot{m}_l}\left\{\frac{(T_l)_i^j-(T_l)_i^{j-1}}{\Delta t}\right\} \tag{4}$$

Here, the subscript *i* denotes general interior node location $i\in[2,N-1]$ and superscript *j* denotes general time step, Δt. Moreover, Δx, Δy and Δz are space steps corresponding to the coordinates *x*, *y* and *z*, respectively. Equations 1-4 represent four coupled partial differential equations. 6 boundary conditions (B.Cs) and 4 initial conditions (I.Cs) are necessary for obtaining the complete solution. In discretised form, these are written below,

$$\text{B.C 1: } I^j A\{1-\alpha_0+\beta_0\ln(\delta)\}+k_n A\left(\frac{\partial T_n}{\partial x}\right)_1^j-\dot{Q}_{rad}^{\ j}-\dot{Q}_{evap}^{\ j}-\dot{Q}_{conv}^{\ j}=\rho_n A\delta c_{pn}\left(\frac{\partial T_n}{\partial t}\right)_1^j$$

$$\text{B.C 2: } I^j A\{\alpha_0-\beta_0\ln(h+\delta)\}-k_n A\left(\frac{\partial T_n}{\partial x}\right)_N^j-$$

$$\dot{m}_f c_{pf}\left\{(T_f)_N^j-T_a^j\right\}+k_g A\left(\frac{\partial T_g}{\partial y}\right)_1^j=\rho_n A dc_{pn}\left(\frac{\partial T_n}{\partial t}\right)_N^j \tag{5}$$

$$\text{B.C 3: } (T_f)_1^j=T_a^j, \quad \text{B.C 4: } (T_l)_N^j=T_a^j$$

$$\text{B.C 5: } (T_n)_N^j=(T_g)_1^j, \quad \text{B.C 6: } (T_g)_N^j=T_{a\_avg}$$

$$\text{I.C 1: } (T_n)_i^1=T_a^1, \quad \text{I.C 2: } (T_f)_i^1=T_a^1, \quad \text{I.C 3: } (T_l)_i^1=T_a^1$$

$$\text{I.C 4: } (T_g)_i^1=T_a^1+\left(\frac{T_{a-avg}-T_a^1}{t_g}\right)\{(i-1).dy\}$$

In the above expressions, *T* denotes temperature, *k* implies thermal conductivity, c_p the specific heat, ρ mass density and *U* the overall heat transfer coefficient across exchanger. Additionally, *N* pertains to the total number of nodal locations for each temperature profile, $\dot{m}$ designates exchanger mass flow rate, *r* represents exchanger pipe radius and *n* signifies number of such pipes in an extraction zone. Subscripts *n*, *f*, *g* and *l* respectively denote NCZ, LCZ exchanger fluid, ground and ground exchanger fluid, respectively. Further, *A* is pond's cross section area, and the four zone thicknesses are designated by δ, *h*, *d*, t_g as shown in Figure 1. Here, temperature has been considered to be in ^oC, whereas, other quantities are taken in their respective Système international (SI) units. In Eq. (5) α_0 and β_0 denote Bryant and Colbeck expression's dimensionless constants describing decay of radiative intensity, *I*. Ambient data of Copiapo, Chile has been taken during the entire study.

The discrete data of solar intensity, ambient temperature, relative humidity and wind speed from the work of Amigo and Suarez [15] have been converted into continuous time functions as indicated below,

$$
\begin{aligned}
I &= 435.3\sin\left\{\left(1.043\times10^{-7}\right)t-0.1402\right\}+305.7\sin\left\{\left(1.928\times10^{-7}\right)t+1.585\right\}+\\
&\quad 74.8\sin\left\{\left(4.216\times10^{-7}\right)t+1.086\right\}+55.23\sin\left\{\left(4.734\times10^{-7}\right)t+3.37\right\}\\
T_a &= 32.13\sin\left\{\left(9.333\times10^{-8}\right)t+0.08217\right\}+19.15\sin\left\{\left(1.655\times10^{-7}\right)t+2.032\right\}+\\
&\quad 17.25\sin\left\{\left(3.803\times10^{-7}\right)t+2.219\right\}+16.55\sin\left\{\left(3.877\times10^{-7}\right)t+5.303\right\}\\
RH &= 0.5197\sin\left\{\left(8.829\times10^{-8}\right)t-0.008827\right\}+0.2696\sin\left\{\left(1.906\times10^{-7}\right)t+1.086\right\}+\\
&\quad 0.04776\sin\left\{\left(5.142\times10^{-7}\right)t+2.318\right\}+0.01991\sin\left\{\left(7.332\times10^{-7}\right)t-0.3721\right\}\\
v_{wind} &= 2.758\sin\left\{\left(1.012\times10^{-7}\right)t-0.1516\right\}+1.567\sin\left\{\left(1.977\times10^{-7}\right)t+1.357\right\}+\\
&\quad 0.3324\sin\left\{\left(4.005\times10^{-7}\right)t+0.7195\right\}+0.0164\sin\left\{\left(6.189\times10^{-7}\right)t-1.085\right\}
\end{aligned}
\tag{6}
$$

In the above expression, RH, T_a and v_{wind} denote relative humidity, ambient temperature and wind speed at time t, respectively. Further, $\dot{Q}_{rad,}\dot{Q}_{evap,}\dot{Q}_{conv}$ denote rate of energy losses from surface at time t due to radiation, evaporation and convection, respectively. These can be computed using standard expressions available elsewhere [14]. Additionally, the overall heat transfer coefficients at the LCZ and ground exchanger surfaces are calculated as suggested by Verma and Das [14]. The implicit finite difference method has been used here with a time step of 1 day and 20 nodes for each of the three temperature fields. These values are found sufficient in generating space and time independent solutions.

Moving forward, the heated water from the two zones is assumed to mix, and fetch a final, output water system. The instantaneous extraction power, P_{ext} can be calculated by using the relevant expression reported in the published literature [13], and temperature of final outgoing stream, T_{out} can be given by the weighted mean of outlet temperatures from the two zones, the weights being respective mass flow rates. Absorption of radiative intensity has been assumed to follow logarithmic decay according to Bryant and Colbeck [16]. The cross-sectional area has been considered to be significantly larger with respect to that of the wall area. Moreover, thermo-fluidic properties of pond water, ground and exchanger fluid (i.e., normal water) have been treated to be invariant with temperature and brine concentration. The pond is assumed to be clear and devoid of any foreign matter.

Table 1: Parameters for validation study of the numerical model

Parameter	Value	Parameter	Value
A	50 m^2	r_f	0.016 m
$\dot{m}_f$	0.05 kg/s	r_l	0.016 m
$\dot{m}_l$	0.05 kg/s	δ	0.2 m
U_f	53.748 W.m^{-2}.^{o}C^{-1}	h	1 m
U_l	100 W.m^{-2}.^{o}C^{-1}	d	0.6 m

3. Validation

Validation has been done with the steady state model of Verma and Das [13] for heat extraction from the LCZ of a solar pond and from neighbouring ground. The parameters required for generating the reference model from the present, more detailed one are given in Table 1. Figure 2 shows satisfactory validation.

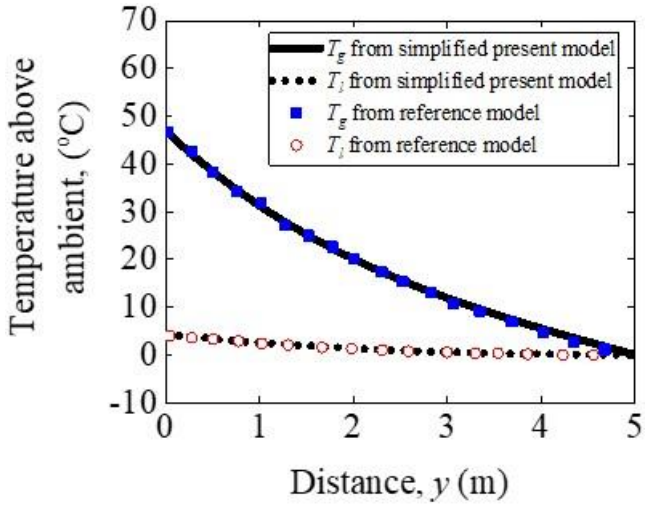

Figure 2: Validation of numerical model with published literature [13]

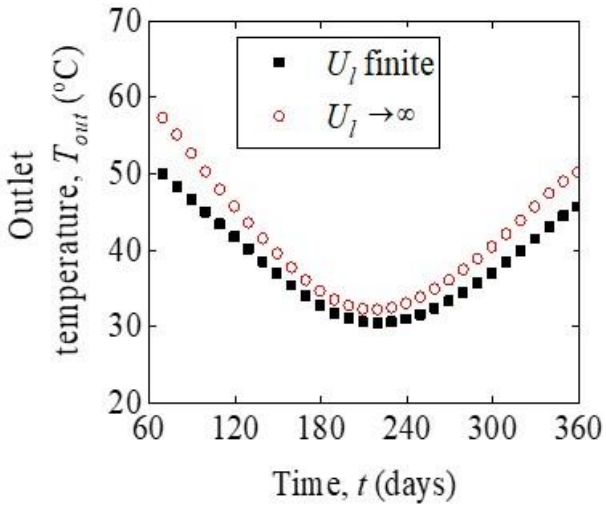

Figure 3: Error due perfect ground extraction assumption; $r_l = 0.02$ m, $\dot{m}_l = 0.05$ kg.s^{-1}, $t_g = 5$ m

4. Results

Figure 3 shows the time evolution of outlet temperature for the present model, and for the special case of zero temperature drop across ground exchanger (available in the literature). It is seen here that the above-mentioned assumption used in the literature overestimates the outlet temperature at every instant. When no temperature drop across ground exchanger is taken into account, it means that maximum possible energy is extracted by it, thus the water stream extracting this energy gets heated to the maximum possible extent, and its temperature also becomes as high as possible. From here, a maximum error of about 13% has been observed in the value of outlet temperature of the extracted water stream due to assumption of ideal heat transfer coefficient. The deviation is found to be least corresponding to minimal value of solar intensity, because lesser radiative intensities would yield lesser local temperatures, and lesser deviations as a consequence. Figure 4 reveals that for a location with larger depth of annual average ambient temperature ground isotherm, outlet temperature increases at every instant as compared to a location with lesser depth of the same. More t_g means a larger distance over which ground extraction transpires, thus it contributes to larger output from ground zone and thus to net output as well. However, the value of t_g depends on the geographical location where pond is built and cannot be manually altered.

Figure 5 suggests that smaller the size of each ground exchanger pipe, the lager will be the outlet temperature for every instant. Heat transfer across ground exchanger is governed by forced convection inside the exchanger pipes. Moreover, as per Dittus-Boelter equation [17], the Nusselt number for the same is a decreasing function of pipe radius. Thus, better heat transfer will be accomplished for smaller pipes. When water is the working fluid flowing through the exchanger pipes, this is not a problem, but when it is air instead, then using smaller pipes drastically raises the power required to pump the same mass flow rate of air. In such cases, effective power, that is, power extracted minus pumping power needs to be the quantity of interest to assess effect of parameters.

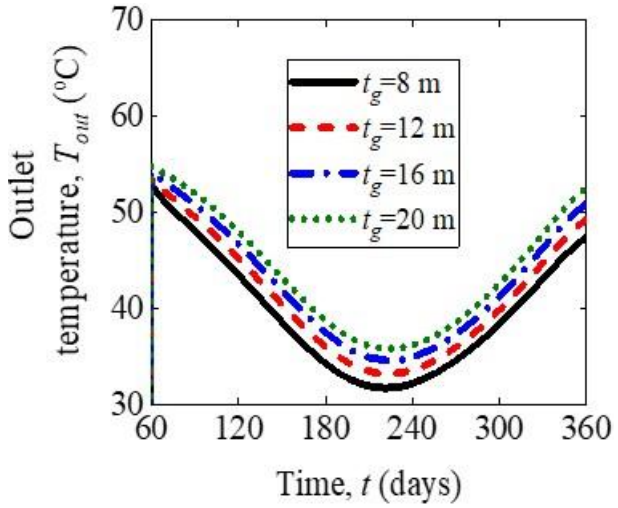

Figure 4: Effect of depth of annual average ambient temperature ground isotherm; $r_l = 0.02$ m, $\dot{m}_l = 0.05$ kg.s^{-1}

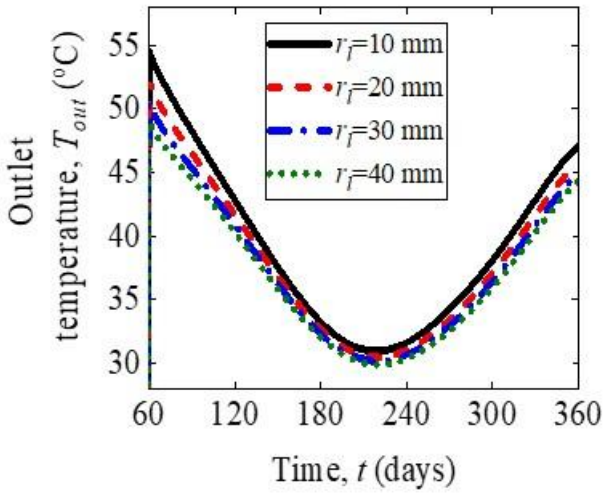

Figure 5: Effect of radius of each ground exchanger pipe; $t_g = 5$ m, $\dot{m}_l = 0.05$ kg.s^{-1}

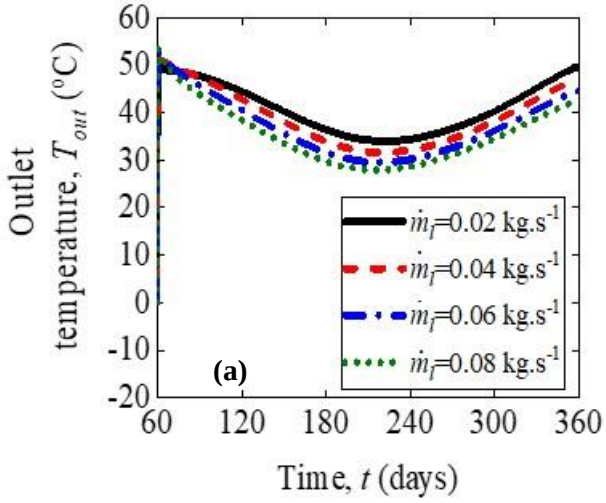

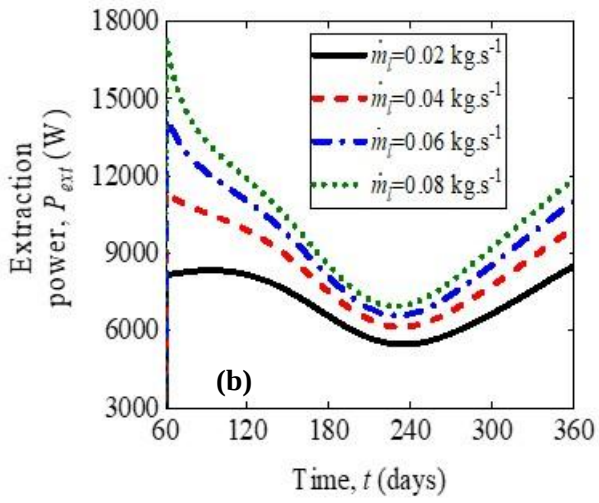

Figure 6: Effect of ground extraction mass flow rate on (a) outlet temperature and (b) power output; $t_g = 5$ m, $r_l = 0.02$ m

Figure 6 shows that a lesser value of ground extraction mass flow rate yields a larger temporal outlet temperature but a lesser temporal extraction power. The value of this parameter depends on the application to which solar pond supplies heat. As an example, suppose energy extracted is used for office space heating. Temperature of this supplied energy must not fall very low, otherwise, the supplied air will not be very hot and may not cause any appreciable comfort conditioning. Simultaneously, it is also desired that a great amount of power is supplied so that the load can be catered well. If power supplied is less at all instants, it is possible that supplied air may not be able to heat up the entire office space, but only a part of it. So suitable values of extraction mass flow rates need to be chosen to strike a balance between these two objectives. If the working fluid flowing within the exchangers is air, then, it would be require more power. So, increasing the mass flow

rate leads to undesirable increase in pumping power, so, in such as case, mass flow rate needs to be chosen in a manner to strike a balance between three considerations, i.e., extracted power, pumping power and outlet temperature.

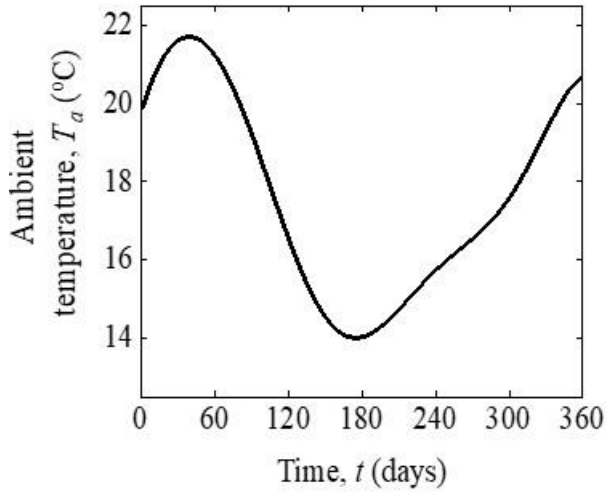

Figure 7: Ambient temperature as a function of time

An interesting finding from Figure 6a is that T_{out} always decreases with time for every value of $\dot{m}_l$ while P_{ext} shows an initial increase for $\dot{m}_l = 0.02$ kg.s^{-1}. This is because P_{ext} is defined as the difference of net outgoing and net incoming power to the pond, whereas T_{out} is calculated as the weighted mean of the outgoing temperatures from the two exchangers, the weights being the respective mass flow rates. Thus, T_{out} is related to only the net outgoing power while P_{ext} is related to both incoming and outgoing powers. The incoming power is function of time as water enters both zones at instantaneous ambient temperature (Fig. 7). Thus, the temporal variation of incoming power can make P_{ext} exhibit a trend different from that of T_{out}.

5. Conclusion

A transient model based on finite differencing scheme is presented to make predictions on a solar pond with realistic energy extraction from ground below as well as its storage zone. Numerical solutions have been acquired for the governing equation and parametric analysis has been performed. The important findings are listed below,

- Assumption of ideal ground energy extraction overestimates outlet temperature from the pond at every moment during operation.
- Deeper annual average ambient temperature ground isotherm is better as it yields greater outlet temperatures throughout the year.
- Radii of ground exchanger pipes should be as small as possible for efficient heat transfer across them.
- Ground extraction mass flux should be lower for greater outlet temperatures, but this will also result in lesser outgoing energy.

This work gives a transient model of a solar pond suffering energy extraction from LCZ and surrounding ground. The authors in a previous work have given a similar model where the two extraction zones were NCZ and LCZ. These two approaches could be combined and a generalized transient model, where all the three zones are considered can be developed as an interesting future study. Further, an economic analysis of the hybrid solar pond and geothermal exchanger system can be performed as a possible extension to this work.

References

[1] S. H. Hammadi, "Integrated solar still with an underground heat exchanger for clean water production," *J. King Saud Univ. Sci.*, vol. 32, no. 5, pp. 339–345, 2020.

[2] M. El Haj Assad, M. H. Ahmadi, M. Sadeghzadeh, A. Yassin, and A. Issakhov, "Renewable hybrid energy systems using geothermal energy: hybrid solar thermal–geothermal power plant," *Int. J. Low-Carbon Technol.*, vol. 16, no. 2, pp. 518–530, 2021.

[3] S. Hu, Z. Yang, J. Li, and Y. Duan, "Thermo-economic optimization of the hybrid geothermal-solar power system: A data-driven method based on lifetime off-design operation," *Energy Convers. Manag.*, vol. 229, pp. 113738, 2021.

[4] Y. Li, T. Long, X. Bai, L. Wang, W. Li, S. Liu, J. Lu, Y. Cheng, K. Ye, and S. Huang, "An experimental investigation on the passive ventilation and cooling performance of an integrated solar chimney and earth–air heat exchanger," *Renew. Energy*, vol. 175, pp. 486–500, 2021.

[5] W. M. Duarte, T. F. Paulino, S. G. Tavares, A. A. T. Maia, and L. Machado, "Feasibility of solar-geothermal hybrid source heat pump for producing domestic hot water in hot climates," *Int. J. Refrig.*, vol. 124, pp. 184–196, 2021.

[6] T. Long, Ningjing Zhao, W. Li, S. Wei, Y. Li, J. Lu, S. Huang, and Z. Qiao., "Numerical simulation of diurnal and annual performance of coupled solar chimney with earth-to-air heat exchanger system," *Appl. Therm. Eng.*, pp. 118851, 2022.

[7] N. W. K. Jayatissa, R. Attalage, P. Hewageegana, P. A. A. Perera, and M. A. Punyasena, "Long Term Stability of an Experimental Insulated-Model Salinity-Gradient Solar Pond," *Int. J. Energy Power Eng.*, vol. 10, no. 2, pp. 319–324, 2016.

[8] A. H. Sayer, H. Al-Hussaini, and A. N. Campbell, "New theoretical modelling of heat transfer in solar ponds," *Sol. Energy*, vol. 125, pp. 207–218, 2016.

[9] S. Verma and R. Das, "Effect of turbidity on choice of zonal thicknesses in solar ponds under various performance evaluation criteria," *J. Clean. Prod.*, vol. 364, pp. 132643, 2022.

[10] S. Verma and R. Das, "Wall energy loss and entropy generation in solar ponds using one-dimensional and two-dimensional transient analyses," *J. Energy Resour. Technol. Trans. ASME.*, vol. 144, no. 10, pp. 101305, 2022.

[11] S. Ganguly, A. Date, and A. Akbarzadeh, "Heat recovery from ground below the solar pond," *Sol. Energy*, vol. 155, pp. 1254–1260, 2017.

[12] S. Verma and R. Das, "Concept of triple heat exchanger-assisted solar pond through an improved analytical model," *J. Sol. Energy Eng.*, vol. 141, no. 5, 2019.

[13] S. Verma and R. Das, "Effect of ground heat extraction on stability and thermal performance of solar ponds considering imperfect heat transfer," *Sol. Energy*, vol. 198, pp. 596–604, 2020.

[14] S. Verma and R. Das, "Transient study of a solar pond under heat extraction from non-convective and lower convective zones considering finite effectiveness of exchangers," *Sol. Energy*, vol. 223, pp. 437–448, 2021.

[15] J. Amigo and F. Suárez, "Ground heat storage beneath salt-gradient solar ponds under constant heat demand," *Energy*, vol. 144, pp. 657–668, 2018.

[16] H. C. Bryant and I. Colbeck, "A solar pond for London?," *Sol. Energy*, vol. 19, no. 3, pp. 321–322, 1977.

[17] Q. Abbas, M.M. Khan, R. Sabir, Y.M. Khan and Z.U. Koreshi, "Numerical simulation and experimental verification of air flow through a heated pipe," *Int. J. Mech. Mechatron. Eng*., vol. 10, pp. 7–12, 2010.